High-Performance WR-4.3 Optically Controlled Variable Attenuator With 60-dB Range

Jun Ren, *Student Member, IEEE*, Zhenguo Jiang, *Student Member, IEEE*, Patrick Fay, *Fellow, IEEE*, Jeffrey L. Hesler, *Member, IEEE*, Cheuk-Yu E. Tong, *Member, IEEE*, and Lei Liu, *Senior Member, IEEE*

***Abstract*— We report the design, fabrication, and characterization of a high-performance optically controlled WR-4.3 variable attenuator. The attenuation is based on the interaction between the incident waves and photogenerated free carriers inside an E-plane micromachined silicon absorber. Tuning is realized by illuminating the silicon with different light intensities using three 808-nm infrared laser diodes. Measurement results show that an average attenuation range of 60 dB, a 0.7-dB insertion loss, and a greater than 15-dB return loss have been achieved over the entire WR-4.3 band. In addition, a 3-dB modulation bandwidth of 350 kHz has been obtained experimentally. Initial thermal stability test of the device has also been performed, with less than 0.4-dB amplitude drift and 2° drift in phase over 30-min demonstration.**

***Index Terms*— Optical tuning, variable attenuators, waveguide.**

I. Introduction

VARIABLE waveguide attenuators are valuable components in many millimeter-wave (mmW)-to-terahertz (THz) sensing, imaging, and communication systems. Applications include THz source leveling, power tuning in balanced mixers or image-rejection receiver systems, and amplitude modulation for synchronous detection (or "chopper") [1], [2]. At present, mechanical devices (e.g., attenuators with movable vanes) are widely used, but these devices typically have low tuning speed, high insertion loss, and limited attenuation range (e.g., a typical commercially available *D*-band attenuator offers 25-dB attenuation range [3]). The implementation of waveguide attenuators at THz frequencies is challenging due to tight machining tolerances and fabrication limitations [2]. Recently, an optically controlled WR-4.3 waveguide attenuator based on the interaction between the propagating waveguide mode and photogenerated free carriers in an *E*-plane micromachined Si absorber illuminated by a laser diode was reported [4], [5]. However, the performance of this prior demonstration suffered from both a limited attenuation range of approximately 25 dB and a strong resonance about 230 GHz that limited the performance.

In this letter, an improved attenuator design has been implemented and characterized. This improved design features a redesigned waveguide block that eliminates the high-frequency resonance. In addition, to enhance the attenuation range, the illuminated area of the Si absorber was increased, and three fiber-coupled laser diodes (instead of one laser in the original design) were used. Furthermore, to reduce the insertion loss, a thin-tapered quartz window was installed along the waveguide sidewall to cover the fiber access holes. In addition to the S-parameter measurement, the device operation speed and thermal stability have also been evaluated. The improved WR-4.3 attenuator shows superior performance, including an average of 60-dB continuous attenuation range, a 0.7-dB insertion loss, a return loss larger than 15 dB, and a 3-dB modulation bandwidth of 350 kHz. The drift of the attenuator was also found to be modest under typical laboratory conditions, with less than 0.4-dB amplitude drift and 2° phase drift over 30 min. The reported variable attenuator is promising for use in a range of mmW–THz systems.

II. Design and Fabrication

The detailed structure of the optically variable WR-4.3 waveguide attenuator is shown in Fig. 1. Its design is based on the interaction between the propagating waveguide mode and photogenerated free carriers in a high-resistivity (20 000 $\Omega \cdot$ cm) Si vane. When illuminated at moderate light intensity, the intrinsic Si becomes a lossy dielectric, resulting in appreciable absorption but yet small reflection of the incident waveguide fields [5]. By varying the light intensity incident on the Si absorber, the dielectric properties of the Si, including conductivity, complex relative permittivity, and loss tangent, can be controlled, and therefore different levels of attenuation can be achieved. Detailed discussion of the operational regimes for this THz attenuation mechanism has been reported previously [4], [5].

As shown in Fig. 1, a 73-μm-thick *E*-plane high-resistivity Si absorbing vane with 4-mm-long tapers at each end (to reduce reflection) is aligned along the waveguide propagation direction in a WR-4.3 waveguide channel. Full-wave HFSS simulations indicated that the high-frequency resonance observed for the device reported in [5] was due to a trapped higher order mode (TE_{11}) propagating in the absorber because the high dielectric constant of the Si absorber ($\varepsilon_r = 11.9$) lowers the cutoff frequency of the higher order mode into

Manuscript received January 12, 2018; revised March 2, 2018; accepted March 28, 2018. This work was supported in part by the National Science Foundation under Grant ECCS-1711631 and Grant ECCS-1711052, and in part by the Harvard-Smithsonian Center for Astrophysics under Grant PTX-Smithsonian 17-SUBC-400SV787007. *(Corresponding author: Jun Ren.)*

J. Ren, Z. Jiang, P. Fay, and L. Liu are with the Department of Electrical Engineering, University of Notre Dame, Notre Dame, IN 46556 USA (e-mail: jren1@nd.edu; zjiang@nd.edu; pfay@nd.edu; lliu3@nd.edu).

J. L. Hesler is with Virginia Diodes, Inc., Charlottesville, VA 22902 USA (e-mail: hesler@vadiodes.com).

C.-Y. E. Tong is with the Harvard-Smithsonian Center for Astrophysics, Harvard University, Cambridge, MA 02138 USA (e-mail: etong@cfa.harvard.edu).

Color versions of one or more of the figures in this paper are available online at http://ieeexplore.ieee.org.

Digital Object Identifier 10.1109/LMWC.2018.2823589

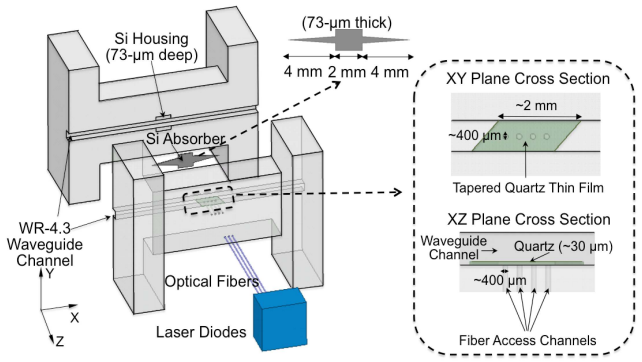

Fig. 1. Schematic of the proposed optically variable WR-4.3 waveguide attenuator.

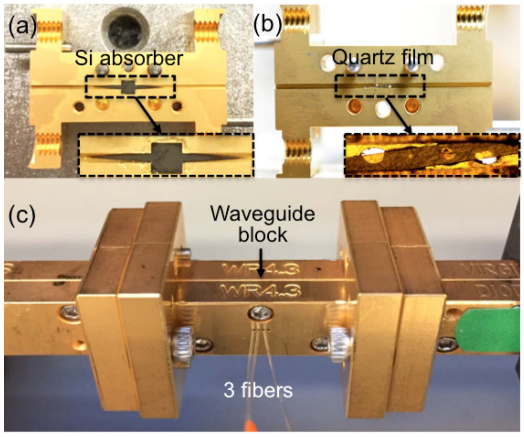

Fig. 2. Photographs of the WR-4.3 optically variable attenuator. (a) Si absorber mounted in the housing cavities. (b) Quartz thin-film window affixed to the sidewall. (c) Assembled waveguide block with three optical fibers inserted.

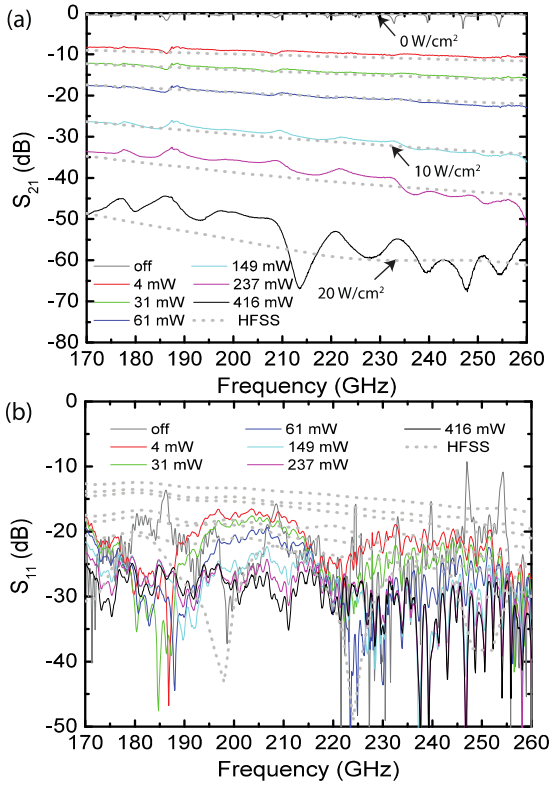

Fig. 3. Measured (solid curve) and simulated (dotted curve) S-parameters ((a) S_{21} and (b) S_{11}) of the variable attenuator as a function of frequency and incident optical power per fiber (corresponding to light intensities of 0, 3.3, 4.8, 6.6, 10, 13.3, and 20 W/cm^2, respectively, in HFSS simulation).

the WR-4.3 band. For the improved design reported here, this high-frequency resonance was eliminated by reducing the depth of the housing cavities from 77 to 73 μm, pushing the TE_{11} mode out of the WR-4.3 band. In addition, the length of the illumination region of the Si absorber was increased to 2 mm. Four fiber access holes with a diameter of 400 ± 25 μm were placed along the narrow wall of the waveguide. In our experiment, only three of them were employed due to the limited availability of high-power laser diodes in our laboratory. From the physics-based model reported in [4] and [5], this configuration is expected to result in a maximum attenuation of 60 dB. To achieve the same level of maximum attenuation, a three-way beam splitter can also be adopted in conjunction with single laser diode. Finally, to prevent the optical fibers from penetrating into the waveguide channel, a 30-μm-thick-tapered quartz window was affixed to the waveguide sidewall to cover the fiber access holes. Since the E-field at the sidewall is minimum, the introduction of the quartz window film will not disturb the waveguide mode significantly. Besides, its low optical and mmW loss allows efficient illumination of the Si without incurring a significant penalty in waveguide loss.

Fig. 2 shows the fabricated prototype. In Fig. 2(a), the Si absorber can be seen. The absorber was fabricated using inductively coupled plasma-reactive ion etching and was mounted in the middle of the housing structure using high thermal conductivity grease. The quartz window was fabricated using a dicing saw and glued to the waveguide sidewall, as shown in Fig. 2(b). The assembled waveguide block with three optical fibers (with an outer diameter of 320 ± 16 μm) fed through the holes on the waveguide sidewall is shown in Fig. 2(c).

III. Characterization and Results

A. Frequency Response

The frequency response of the prototype attenuator was characterized using a Keysight N5245A PNA-X (VNA) along with two WR-4.3 extenders from Virginia Diodes, Inc., (VDI), Charlottesville, VA, USA. To control the attenuation, the Si absorber was illuminated by three fiber-coupled 808-nm laser diodes (QPhotonics, QSP-808-4). The lasers were powered by three dc power supplies; all three lasers were set to the same drive current level. Fig. 3 shows the measured device S-parameters versus frequency as a function of incident optical power per fiber. The optical power from the fiber at each drive current level was characterized using an ILX Lightwave OMM-6810B optical multimeter in conjunction with an OMH-6722B measurement head before the actual measurement of the attenuator device. As can be seen in Fig. 3(a), an average insertion loss of 0.7 dB was measured when all the lasers are OFF ("OFF" curve). The small spikes on the measured S_{21} curves arise from the imperfect flange mating due to the deformed flange structures of the waveguide block. As the illumination intensity increases, the attenuation also increases. For optical power (per fiber) from 0 to 416 mW, the attenuation can be continuously tuned with an

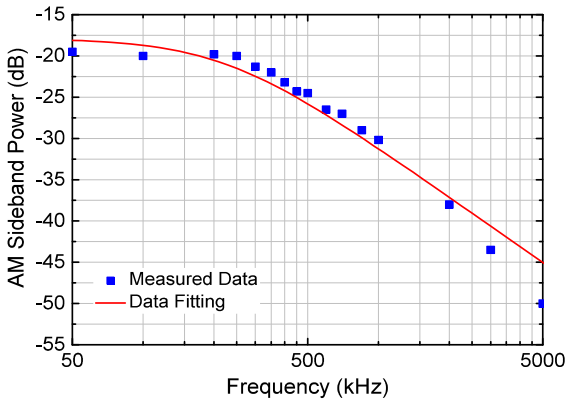

Fig. 4. Measured sideband power (blue square) of the modulated signal for a carrier frequency of 225 GHz and data-fitting results (red curve). The 350-kHz operation speed has been demonstrated.

average attenuation control range (across the WR-4.3 band) of approximately 60 dB. Fig. 3(b) shows the measured S_{11}, demonstrating that over 15-dB return loss is achieved over the entire WR-4.3 band under all the illumination conditions. No indications of resonances are seen, indicating that the TE_{11} mode has been adequately suppressed in the improved design.

Simulated S-parameters as a function of light intensity are also presented in Fig. 3. In these simulations, the Si absorber is treated as a lossy dielectric with conductivity in the illuminated regions (1.5 mm long in total with each fiber contributing a 0.5-mm-long illumination spot) determined using the physics-based model in [4] and [5]. Considering surface recombination and bulk defect density, a carrier lifetime of 0.5 μs (also verified by modulation bandwidth testing in Section III-B) was utilized in this calculation. As observed in Fig. 3, good agreement between measurement and simulation has been obtained. A light intensity of 20 W/cm^2 was found to match the attenuation level for 416-mW optical power per fiber, which indicates an optical power coupling efficiency of 28.3% (in good agreement with the previously reported result [5]). Higher efficiency can be achieved by engineering the thickness of the quartz thin-film window for optical matching.

B. Modulation Bandwidth

The modulation bandwidth of the attenuator was also evaluated. Using a single laser at a dc power level of 83.3 mW, a low-frequency ac modulation was added to the laser drive current using a Stanford Research DS345 signal generator and a Marki BT-0018 bias tee. A 225-GHz continuous-wave signal was supplied to the attenuator under test, and the output was monitored using an HP8563E spectrum analyzer in conjunction with a VDI WR-3.4 EHM harmonic mixer. As the modulation signal generator frequency was increased from 50 to 5000 kHz, the depth of modulation was measured by observing the power ratio of the 225-GHz carrier to the sideband caused by the modulation. Fig. 4 shows the measured data as well as the least-squares fit to a single-pole transfer function. As shown in Fig. 4, the 3-dB modulation bandwidth is 350 kHz. This bandwidth is in good agreement with a theoretical expectation of 318 kHz for an intrinsic Si absorber with a carrier lifetime of 0.5 μs [6].

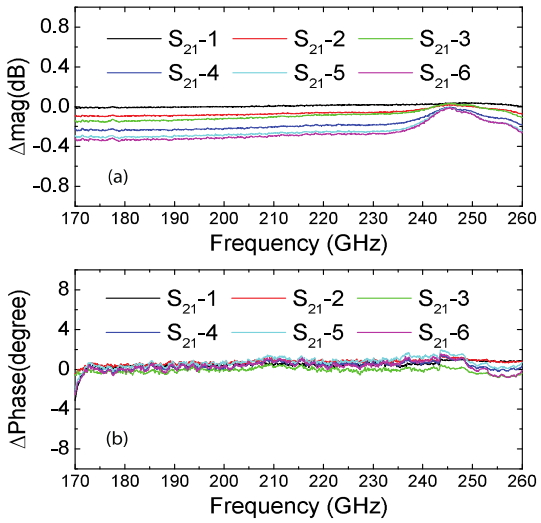

Fig. 5. (a) Magnitude and (b) phase drift of the S-parameter (S_{21}, reference set at the beginning of each measurement) under 1.2-A driving current.

C. Stability Testing

Stability is a critical performance metric for variable attenuators. To evaluate the stability of the attenuator, S-parameters were measured and recorded with single laser diode on every 5 min over a span of 30 min in an approximate 23 °C laboratory environment. During the measurement, the laser drive current held constant at 1.2 A (corresponding to 149-mW power), and the temperature of the diode was recorded, which showed less than 0.5 °C variation over the course of 30 min. The measured S_{21} traces are shown in Fig. 5. Less than 0.4-dB magnitude drift and smaller than 2° phase drift were observed over the entire testing period.

IV. Conclusion

An optically controlled variable WR-4.3 waveguide attenuator has been designed, fabricated, and characterized. Excellent performance, including an average of 60-dB continuous attenuation range, a 0.7-dB insertion loss, a greater than 15-dB return loss, and a 350-kHz modulation bandwidth, has been demonstrated. In addition, preliminary thermal stability test of the device has also been performed, showing less than 0.4-dB amplitude drift and 2° drift in phase over 30 min. The demonstrated attenuator is promising for applications in a range of mmW–THz systems.

References

[1] J. Li and J. Yao, "Controllable terahertz wave attenuator," *Microw. Opt. Technol. Lett.*, vol. 50, no. 7, pp. 1810–1812, 2008.

[2] S. Biber, D. Schneiderbanger, and L.-P. Schmidt, "Design of a controllable attenuator with high dynamic range for THz-frequencies based on optically stimulated free carriers in high-resistivity silicon," *Frequenz*, vol. 59, nos. 5–6, pp. 141–144, 2005.

[3] *Millitech Product Specifications*. Accessed: Oct. 10, 2017. [Online]. Available: http://www.millitech.com/MMW-PassiveWaveguide Component-LSA-FXA-VPS.htm

[4] A. Kannegulla, M. I. B. Shams, L. Liu, and L.-J. Cheng, "Photo-induced spatial modulation of THz waves: Opportunities and limitations," *Opt. Exp.*, vol. 23, no. 25, pp. 32098–32112, 2015.

[5] Z. Jiang *et al.*, "Investigation and demonstration of a WR-4.3 optically controlled waveguide attenuator," *IEEE Trans. THz Sci. Technol.*, vol. 7, no. 1, pp. 20–26, Jan. 2017.

[6] H. Alius and G. Dodel, "Amplitude-, phase-, and frequency modulation of far-infrared radiation by optical excitation of silicon," *Infr. Phys.*, vol. 32, no. 1, pp. 1–11, 1991.